

Duality transformation between hole arrays and wire networks in superconducting Nb films

S. K. He, W. J. Zhang, H. F. Liu, G. M. Xue, B. H. Li, H. Xiao,
Z. C. Wen, X. F. Han, S. P. Zhao, C. Z. Gu, and X. G. Qiu*
*Beijing National Laboratory for Condensed Matter Physics,
Institute of Physics, Chinese Academy of Science, Beijing 100190, China*

We present transport measurements on superconducting Nb films with periodic hole arrays. The arrays are honeycomb and kagomé lattices with edge-to-edge separation between nearest neighboring holes comparable to the coherence length at temperature close to T_{c0} . Fine structures in the field dependent resistance $R(H)$ and transition temperature $T_c(H)$ curves are observed in both arrays. Comparison of experimental data with calculation results shows that these structures resemble those observed in wire networks with triangular and T_3 symmetries, whose dual are honeycomb and kagomé, respectively. A duality transformation between hole arrays and wire networks has been established. Our results suggest that in these specified periodic hole arrays the physics associated with the fine structures is dominated by that in wire networks.

PACS numbers: 74.25.F-, 74.78.Na, 74.81.Fa

I. INTRODUCTION

Superconducting films with periodic arrays of artificial pinning sites have been extensively studied in the past two decades.¹⁻⁴ It is found that at the matching fields where the number of superconducting flux quantum $\Phi_0 = hc/2e$ in unit area is an integer multiple of the density of pinning sites, the so called commensurate effects such as peaks in the $I_c(H)$ and dips in the $R(H)$ curves can be observed.^{3,5,6} The most prevailing explanation for these commensurate effects is that the vortex lattice commensurates with the underlying array and is pinned efficiently at the matching fields. According to this point of view, ordered vortex lattice leads to enhanced critical current at the matching fields, resulting in the commensurate effects.

However, similar phenomena have also been observed in other periodic systems including superconducting wire networks and Josephson junction arrays.⁷⁻⁹ In wire networks, when the magnetic flux through a single plaquette does not equal to integer multiple of Φ_0 , the fluxoid quantization condition requires supercurrent to be induced along the loops, resulting in a reduced T_c . Therefore, for the wire networks, the commensurate effects are a result of the T_c suppression at incommensurate fields rather than enhanced pinning at matching fields. By comparing the $R(H)$ and $T_c(H)$ results obtained in perpendicular and parallel field directions, U. Patel *et al.*¹⁰ argued that even in hole arrays, T_c suppression at non-matching fields can sometimes give rise to the resistance oscillations. A natural question one will ask is if we can correlate the wire networks and hole arrays showing similar behaviors. For periodic hole arrays, with increasing hole diameter, the width of the strips between neighboring holes become comparable to the coherence length at temperatures close to T_{c0} (zero resistance transition temperature). It is expected that the behavior of the system may show a transition from the pinning arrays to

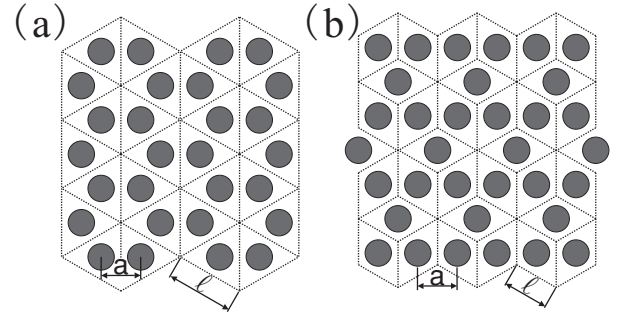


FIG. 1: Illustration of the transformation from hole arrays (dark circles) to wire networks (dotted lines). (a) Honeycomb hole array to triangular wire network. (b) Kagomé hole array to T_3 wire network. a : the distance between the centers of the neighboring holes. l : the side length of the corresponding wire networks.

those of wire networks.^{3,11,12} It has been found that in hole arrays showing wire network behavior, qualitatively different type of integer matching anomaly in magnetization curves¹² and many more oscillation periods in $R(H)$ curves³ were observed. We notice that a wire network is obtained by assigning nodes to the center of the interstitial regions in the original hole array and connecting them. In Fig. 1, the centers of the interstitial regions are regarded as nodes. Then, the superconducting stripes between neighboring holes are viewed as wires (dotted lines) connecting the nodes. Following this procedure, the connectivity of the patterned films are highlighted and the honeycomb and kagomé hole arrays are transformed to triangular and T_3 wire networks, respectively. In other words, there exists a so called duality transformation between a hole array and its corresponding wire network. Assuming that the distance between the centers of the neighboring holes is a in the hole array, then in the dual lattices the side length l of the elementary triangles will be $\sqrt{3}a$ and the side length of the rhombus tile in

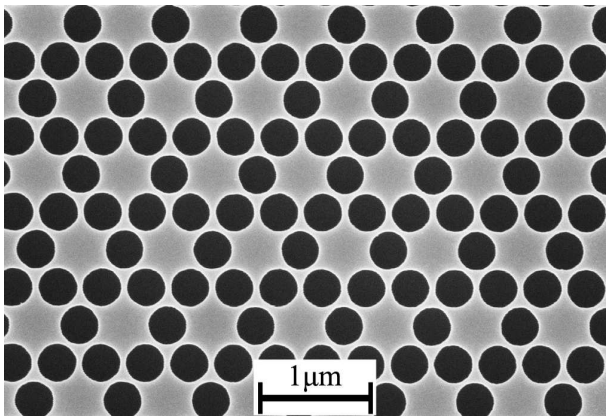


FIG. 2: Scanning electron microscopy (SEM) image of the superconducting Nb film with kagomé hole array. The distance between the centers of the neighboring holes is about 400 nm and the hole diameter is about 340 nm.

the T_3 geometry will be $2\sqrt{3}a/3$ as can be seen from Fig. 1(a) and Fig. 1(b), respectively. If the matching effects of the hole arrays originate from T_c suppression at non-matching fields, the experimental results should show similar features with what have been observed in their dual wire networks.

In the present paper, we report transport measurements on superconducting Nb films with honeycomb and kagomé array of holes. The edge-to-edge separation between neighboring holes in these samples are comparable to the coherence length at temperature close to T_{c0} . We focus on the fine structures (fractional matchings) in $R(H)$ and $T_c(H)$ curves. We find that these fine structures are the fingerprints which can identify the similarity between hole arrays and wire networks. The comparison with those of their dual wire networks, including reported experimental data as well as calculation results based on the Alexander model,¹³ demonstrates that there is a good duality transformation between hole array and wire network.

II. EXPERIMENT

The nano-structured superconducting films were prepared as follows. First, the superconducting Nb film with a thickness of 100 nm was deposited by magnetron sputtering on Si substrate with SiO₂ buffer layer. Next, micro-bridge for four terminal transport measurement was fabricated by ultraviolet photolithography followed by reactive ion etching. Then the desired arrays covering the whole bridge area of $60 \times 60 \mu\text{m}^2$ was patterned by electron-beam lithography on a polymethyl methacrylate (PMMA) resist layer. Finally the pattern was transferred to Nb film by magnetically enhanced reactive ion etching. In both the honeycomb and kagomé samples, the value of a is 400 nm and the hole diameter of about 340 nm. Scanning electron micrograph image

of the kagomé sample is shown in Fig. 2. The smallest width of the stripes between the adjacent holes is only about 60 nm, the diameter of the disk-shaped interstitial region is about 500 nm. We have chosen honeycomb and kagomé hole arrays for the following reasons. First, unlike square and triangular arrays, even when the width of the superconducting strips between neighboring holes are comparable to the coherence length, our patterned films still have large interstitial regions which makes the dual transformation more subtle. The second reason is that kagomé (and its dual, the so called T_3) wire networks show distinct destructive quantum interference at half flux quantum per tile^{14,15} which is rather different from arrays with other symmetry and can be used to further test the duality relation. Furthermore, some geometrically frustrated magnetic systems have kagomé lattice, it is possible that the phenomena observed in our work and the duality transformation method can be helpful to understand the physics associated with frustration in these systems and etc..

The transport measurements were carried out in a commercial Physical Properties Measurement System (PPMS) manufactured by Quantum Design. The magnetic field was applied perpendicular to the film surface. During the measurements, the temperature stability was better than 2 mK. The zero field transition temperature $T_c(0)$ are 8.713 K for honeycomb sample and 8.755 K for kagomé sample, using a criterion of half the normal state resistance R_N at 9 K, which are 8.18 Ω and 9.02 Ω , respectively. The transition width of these two samples is about 0.15 K. Reference film without any pattern has a slightly higher T_c of 8.87 K and transition width of 50 mK. We have measured the $T_c(H)$ phase boundary of the reference sample and obtained the zero-temperature coherence length $\xi(0) = 9.9 \text{ nm}$.¹⁶

III. RESULTS AND DISCUSSION

Figure 3(a) shows the normalized $R(H)$ curve of the honeycomb sample measured at 8.60 K. The x axis is given as filling ratio, $f = \Phi/\Phi_0$, where $\Phi = Ha^2\sqrt{3}/4$ is the magnetic flux per elementary triangle of the corresponding dual wire network. In the field range $0 \leq f \leq 1$, resistance minima are observed at $f=1/4, 1/3, 1/2, 2/3$ and $3/4$. The magnitude of the oscillation is about eight percent of R_N . At the field $f=1/2$ where the commensurate effect is most pronounced, the resistance drops to a value comparable to that at zero field. At $f=1/4$ and $3/4$, the resistances are about four percent of R_N .

Figure 3(b) shows the $T_c(H)$ curves in reduced units, $\Delta T_c/T_c(0)$ vs f , using different resistance criteria $r = R/R_N$. The parabolic background has been subtracted following a common procedure.⁷ For $r=0.05$ and 0.1, dips are observed at filling ratios $f=1/4, 1/3, 1/2, 2/3$ and $3/4$. With the criterion of $r=0.5$, only dips at $f=1/4, 1/2$ and $3/4$ are visible and those at $f=1/3$ and $2/3$ are missing. For $r=0.8$, T_c changes smoothly with field and no features

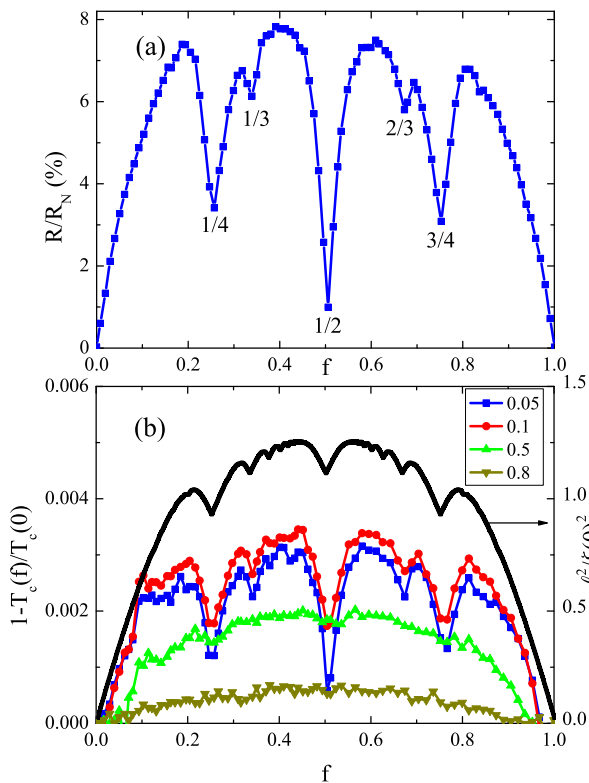


FIG. 3: (Color online) (a) Reduced $R(H)$ curve for the sample with a honeycomb hole array measured at 8.60 K and $I=10 \mu\text{A}$. The field is normalized by the first matching field and the resistance is normalized by R_N at 9 K. (b) The field dependent transition temperature $T_c(H)$ curves of the honeycomb sample with different criteria $r = R/R_N$. The parabolic background has been subtracted. The top one is the theoretical curve for triangular wire network in unit of $l^2/\xi(0)^2$.

can be identified. Thus, comparing Fig. 3(a) and (b), one can see that minima in the $R(H)$ curve locate at the same fields where dips are observed in the $T_c(H)$ curve. The fine structures are more pronounced in $R(H)$ than in $\Delta T_c/T_c(0)$ vs f . This is because the resistance is measured at temperatures slightly above T_{c0} in the superconducting transition region where resistance drops sharply with decreasing temperature, a small change in T_c will result in an enhanced effect in resistance, and thus a more pronounced commensurate effect.

To our knowledge, fractional matching effect in honeycomb arrays have only been observed at $f=1/2$ in previous studies.^{17,18} At the typical measuring temperature $T=0.99T_c$ in this work, $\xi(T)=\xi(0)/\sqrt{1-T/T_c}=99 \text{ nm}$ is larger than the width of the narrow stripes. This fact makes the samples investigated here be qualitatively different from those in previous works on hole arrays and be better described as wire networks. Besides integer matchings, rich structures are usually observed in the $T_c(H)$ curves.⁷ These are fingerprints to differentiate one array from another since for a given geometry the fine structures are only expected at a particular series of filling

ratios.^{19,20} From the linearized Ginzburg-Landau equations, Alexander derived the relation of the order parameters at the nodes subjected to non-integer flux.¹³ Based on those equations, the task of finding the field dependent transition temperature is reduced to eigenvalue problems. The mathematical treatment is very similar to that of the tight bounding electrons in 2D arrays subjected to an external field which leads to the famous Hofstadter butterfly energy spectrum.²¹ The top curve plotted in Fig. 3(b) is the theoretical values of $T_c(H)$ for the triangular wire network, the dual lattice of honeycomb hole array, which is calculated by

$$\frac{T_c(0) - T_c(f)}{T_c(0)} = \frac{\xi(0)^2}{l^2} \left(\arccos \frac{\varepsilon_t}{6} \right)^2, \quad (1)$$

where l is the side length of the wires, ε_t is the eigenvalue¹³ of the following equation obtained by using Landau gauge and periodic boundary conditions,

$$\begin{aligned} \varepsilon_t \psi_n &= 2 \cos[\pi(2n-1)f - k_y/2] e^{-ik_y/2} \psi_{n-1} \\ &+ 2 \cos[4\pi n f - k_y] \psi_n \\ &+ 2 \cos[\pi(2n+1)f - k_y/2] e^{ik_y/2} \psi_{n+1}, \end{aligned} \quad (2)$$

where $k_y = 2\pi \frac{k-1}{N}$, $k = 1, \dots, N$ implies the periodic condition, n denotes the node index and ψ_n is the order parameter at node n . The fine structures of the $T_c(H)$ of triangular wire network have also been studied by analytical approach based on multiple-loop Aharonov-Bohm Feynman path integrals.¹⁹ The main features in $T_c(H)$ such as the position and relative strength of the most prominent dips are the same as those in the Alexander's treatment. The most pronounced dips occur at $f=1/4, 1/3, 1/2$ etc., in good agreement with the experimental data. At the fields where dips are observed, the order parameter at the nodes interferences constructively and form different locked-in states corresponding to local maxima in T_c .¹⁵

Figure 4(a) is the $R(H)$ curve of the kagomé sample measured at 8.67 K. With kagomé geometry, f corresponds to the magnetic flux through a rhombic tile with side length $2\sqrt{3}a/3$: $f = \Phi/\Phi_0 = 2\sqrt{3}a^2 H/(3\Phi_0)$. Again we focus on the results for f in the interval between 0 and 1. Dips are identified at $f=1/6, 2/9, 7/9$ and $5/6$. These fine structures are observed for the first time in kagomé hole array, perhaps because of the specified geometrical parameters adopted here. Anomalies are also visible at $f=1/3$ and $2/3$, but they are more like kinks than dips. Most strikingly, in contrast to the dip observed in the honeycomb sample, a remarkable peak is observed at $f=1/2$. The resistance is far above the background, reaches 16.9 percent of the normal state resistance.

Figure 4(b) shows the $T_c(H)$ curve in reduced units, $\Delta T_c/T_c(0)$ vs f , of the kagomé sample determined by using different criteria of r . For small value of r (0.05 and 0.1), dips present at $1/6, 2/9, 1/3, 2/3$ and $5/6$, although the one at $2/3$ is relatively weak (see the labels

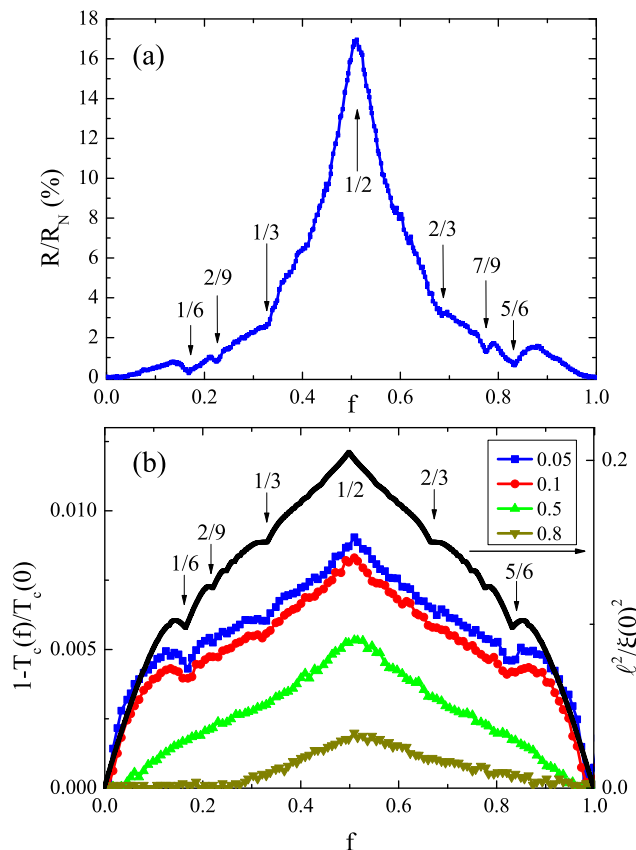


FIG. 4: (Color online) (a) Reduced $R(H)$ curve for sample with kagomé array measured at 8.67 K and $I=10 \mu\text{A}$. (b) The field dependent transition temperature $T_c(H)$ of the kagomé sample with different criteria $r = R/R_N$. The parabolic background has been subtracted. The top one is the theoretical curve for T_3 wire network (Ref. 14) in unit of $l^2/\xi(0)^2$.

in Fig. 4(b)). For larger values of r (0.5 and 0.8), the dips at $1/6$, $2/9$ and $1/3$ gradually disappear but the peak at $f=1/2$ remains pronounced.

Most of the fractional matchings observed here are absent in previous works performed on kagomé lattice for the study on the vortex dynamics.^{18,22–25} In a recent work on hole arrays with small hole size which is in the pinning regime limit, clear fractional matchings were only observed at $f=1/3$ and $2/3$.²⁵ Contrasting to their findings, in our work with edge-to-edge separation comparable to the coherence length, dips at $f=1/6$ and $5/6$ are most pronounced and a distinct peak anomaly at $f=1/2$ is observed. The results agree well with what have been observed in T_3 wire networks,^{14,26} the dual of kagomé as seen in Fig. 1(b). The top curve of Fig. 4(b) shows the theoretical curve of T_3 networks.¹⁴ This is done by the following equation which relates the eigenvalues of T_3 ($\varepsilon(f)$) at filling ratio f to the eigenvalues for triangular lattice at $3f/2$.¹⁴

$$\varepsilon^2(f) - 6 = 2 \cos(\pi f) \varepsilon_t(3f/2) \quad (3)$$

The comparison with the theoretical curve show that only

the dips at $7/9$ and weaker ones are absent in the experimental curves. For $f=1/6$, $2/9$ and $1/3$, constructive interference occurs among the superconducting order parameters of the interstitial sites and the fluxoids establish long range locked-in commensurate order. While for $f=1/2$, superconductivity is localized in single tiles and long range coherence between network sites cannot be established.¹⁴ This kind of fully destructive quantum interference has also been observed in T_3 's dual, kagomé wire networks^{15,27}. The oscillation of $R(H)$ curve with a peak at half a flux per tile is similar to the single-loop Little-Parks effect. In that case, the supercurrent density reaches the largest value at half flux in order to satisfy the fluxoid quantization condition.²⁸

The results obtained from these two lattices are consistent with the expectation that the hole arrays with small edge-to-edge separation should behave like wire networks. However, some differences between the arrays and the wire networks are obvious. In the geometries studied here, there are large superconducting disk-shaped interstitial region connected by the wires, in contrast to the small nodes in ideal wire networks. Because the interstitial regions have diameters about ten times larger than the coherence length, at larger fields Abrikosov vortices will be nucleated and trapped there.^{17,18} The formation of Abrikosov vortices implies spatial variation and presence of zeros of the order parameters in the interstitial region. Then the simplification of the large interstitial region into a node in a wire network is no longer appropriate. Therefore duality transformation from hole arrays to wire networks is only valid for small field values when no interstitial vortex is involved.

Duality transformation is a very useful method to relate the physical properties of one system to those of another, simplifies the treatment of one system, helps understanding the phenomenon in a relatively complicated system and provides new physical understanding.²⁹ It has been applied successfully to the two dimensional Ising model for interacting magnetic spins to treat models with different interactions at different temperatures. It has also been applied to study the fractional quantum hall effect liquid state of the two-dimensional electron system.³⁰ In the case studied here, we have established duality transformation between hole arrays and wire networks based on our results. The simple method of the dual transformation can apply to other kind of hole arrays. We are aware that although without mentioning duality, C. C. Abilio *et al.* have found that superconducting Al film with a square array of holes can be described as a square wire network, i.e., they are self-dual.³¹ While the analytical treatment for hole arrays are complicated because of the boundaries at each hole, the methods to understand physics in wire networks are well developed. Therefore, this duality transformation provides a simple way to understand physics in some specified hole arrays. Furthermore, the macroscopic quantum state nature of superconductivity and the tunability of the interactions between fluxoids in these artificial lattices by applied

magnetic field and temperature can also possibly provide a model system in studying related phenomena in interacting magnetic systems.

IV. CONCLUSION

In conclusion, we have studied the commensurate effects in $R(H)$ and $T_c(H)$ of honeycomb and kagomé hole arrays. At small field values when no Abrikosov vortices presents in the interstitial regions, the shapes of the curves and the position of the dips are in good agreement with what have been observed in triangular and T_3 wire networks. From the comparison of the fine structures we have established a duality transformation between the

hole arrays and wire networks. The theoretical treatments for wire networks is more convenient than that for hole arrays, this duality provides a way to treat phenomena in hole arrays with small edge-to-edge separation.

V. ACKNOWLEDGEMENTS

We thank Q. Niu, X. C. Xie, V. V. Moshchalkov, B. Y. Zhu and Y. Yeshurun for fruitful discussion. This work is supported by National Basic Research Program of China(No.2009CB929100,2011CBA00107,2012CB921302) and National Science Foundation of China (No. 10974241).

-
- * xgqiu@aphy.iphy.ac.cn
- ¹ M. Baert, V. V. Metlushko, R. Jonckheere, V. V. Moshchalkov, and Y. Bruynseraede, Phys. Rev. Lett. **74**, 3269 (1995).
 - ² J. I. Martin, M. Velez, A. Hoffmann, I. K. Schuller, and J. L. Vicent, Phys. Rev. Lett. **83**, 1022 (1999).
 - ³ A. Hoffmann, P. Prieto, and I. K. Schuller, Phys. Rev. B **61**, 6958 (2000).
 - ⁴ G. Karapetrov, J. Fedor, M. Iavarone, D. Rosenmann, and W. K. Kwok, Phys. Rev. Lett. **95**, 167002 (2005).
 - ⁵ L. Van Look, B. Y. Zhu, R. Jonckheere, B. R. Zhao, Z. X. Zhao, and V. V. Moshchalkov, Phys. Rev. B **66**, 214511 (2002).
 - ⁶ J. I. Martin, M. Velez, J. Noguez, and I. K. Schuller, Phys. Rev. Lett. **79**, 1929 (1997).
 - ⁷ B. Pannetier, J. Chaussy, R. Rammal, and J. C. Villegier, Phys. Rev. Lett. **53**, 1845 (1984).
 - ⁸ X. S. Ling, H. J. Lezec, M. J. Higgins, J. S. Tsai, J. Fujita, H. Numata, Y. Nakamura, Y. Ochiai, C. Tang, P. M. Chaikin, et al., Phys. Rev. Lett. **76**, 2989 (1996).
 - ⁹ M. Tinkham, D. W. Abraham, and C. J. Lobb, Phys. Rev. B **28**, 6578 (1983).
 - ¹⁰ U. Patel, Z. L. Xiao, J. Hua, T. Xu, D. Rosenmann, V. Novosad, J. Pearson, U. Welp, W. K. Kwok, and G. W. Crabtree, Phys. Rev. B **76**, 020508 (2007).
 - ¹¹ Y. Bruynseraede, T. Puig, E. Rosseel, M. Baert, M. Van Bael, K. Temst, V. Moshchalkov, and R. Jonckheere, J. Low Temp. Phys. **106**, 173 (1997).
 - ¹² V. V. Moshchalkov, M. Baert, V. V. Metlushko, E. Rosseel, M. J. Van Bael, K. Temst, Y. Bruynseraede, and R. Jonckheere, Phys. Rev. B **57**, 3615 (1998).
 - ¹³ S. Alexander, Phys. Rev. B **27**, 1541 (1983).
 - ¹⁴ C. C. Abilio, P. Butaud, T. Fournier, B. Pannetier, J. Vidal, S. Tedesco, and B. Dalzotto, Phys. Rev. Lett. **83**, 5102 (1999).
 - ¹⁵ M. J. Higgins, Y. Xiao, S. Bhattacharya, P. M. Chaikin, S. Sethuraman, R. Bojko, and D. Spencer, Phys. Rev. B **61**, R894 (2000).
 - ¹⁶ M. Tinkham, *Introduction to Superconductivity* (McGraw-Hill, New York, 1975).
 - ¹⁷ T. C. Wu, J. C. Wang, L. Horng, J. C. Wu, and T. J. Yang, J.Appl.Phys. **97**, 10B102 (2005).
 - ¹⁸ C. Reichhardt and C. J. O. Reichhardt, Phys. Rev. B **76**, 064523 (2007).
 - ¹⁹ Y.-L. Lin and F. Nori, Phys. Rev. B **65**, 214504 (2002).
 - ²⁰ P. Erdős and W. Zheng, Phys. Rev. B **82**, 134532 (2010).
 - ²¹ D. R. Hofstadter, Phys. Rev. B **14**, 2239 (1976).
 - ²² D. J. Morgan and J. B. Ketterson, Phys. Rev. Lett. **80**, 3614 (1998).
 - ²³ M. F. Laguna, C. A. Balseiro, D. Domínguez, and F. Nori, Phys. Rev. B **64**, 104505 (2001).
 - ²⁴ C. Reichhardt and C. J. Olson Reichhardt, Phys. Rev. B **79**, 134501 (2009).
 - ²⁵ J. Cuppens, G. W. Ataklti, W. Gillijns, J. Van de Vondel, V. V. Moshchalkov, and A. V. Silhanek, J Spercond Nov Magn **24**, 7 (2011).
 - ²⁶ J. Vidal, R. Mosseri, and B. Douçot, Phys. Rev. Lett. **81**, 5888 (1998).
 - ²⁷ Y. Xiao, D. A. Huse, P. M. Chaikin, M. J. Higgins, S. Bhattacharya, and D. Spencer, Phys. Rev. B **65**, 214503 (2002).
 - ²⁸ W. A. Little and R. D. Parks, Phys. Rev. Lett. **9**, 9 (1962).
 - ²⁹ S. M. Girvin, Science **274**, 524 (1996).
 - ³⁰ D. Shahar, D. C. Tsui, M. Shayegan, E. Shimshoni, and S. L. Sondhi, Science **274**, 589 (1996).
 - ³¹ C. Abilio, L. Amico, R. Fazio, and B. Pannetier, J. Low Temp. Phys. **118**, 23 (2000).